

# Using Trimethylphosphine as a Probe Molecule to Study the Acid Sites in Al–MCM-41 Materials by Solid-State NMR Spectroscopy

Qing Luo,<sup>†</sup> Feng Deng,<sup>\*,†</sup> Zhongyong Yuan,<sup>‡</sup> Jun Yang,<sup>†</sup> Mingjin Zhang,<sup>†</sup> Yong Yue,<sup>†</sup> and Chaohui Ye<sup>†</sup>

State Key Laboratory of Magnetic Resonance and Atomic and Molecular Physics, Wuhan Institute of Physics and Mathematics, Chinese Academy of Science, Wuhan 430071, People's Republic of China, and Beijing Laboratory of Electron Microscopy, Institute of Physics and Center for Condensed Matter Physics, Chinese Academy of Science, Beijing 100080, People's Republic of China

Received: May 30, 2002

Using trimethylphosphine (TMP) as a probe molecule, acid sites in a series of Al–MCM-41 materials with Si/Al ratios ranging from 16 to 80 were investigated by various solid-state NMR techniques including  $^{29}\text{Si}$ ,  $^{31}\text{P}$ ,  $^{27}\text{Al}$ ,  $^1\text{H}$  magic-angle spinning (MAS), and some double- or triple-resonance methods such as  $^{31}\text{P} \rightarrow ^1\text{H}$  cross polarization (CP),  $^1\text{H}/^{27}\text{Al}$ , and  $^1\text{H}/^{31}\text{P}/^{27}\text{Al}$  TRAPDOR (transfer of population in double resonance). By means of the  $^1\text{H}/^{27}\text{Al}$  TRAPDOR technique, which has the ability to establish a correlation between  $^1\text{H}$  and  $^{27}\text{Al}$ , the hydroxyl groups associated with Al could be discriminated from the silanol groups. Two signals at 3.5 and 1.9 ppm were observed in the  $^1\text{H}/^{27}\text{Al}$  TRAPDOR spectra; they are likely due to the bridging hydroxyl (SiOHAl) and aluminum hydroxyl groups, respectively.  $^{31}\text{P}$  MAS NMR strongly supports the formation of zeolitelike Brönsted acid sites in the mesoporous material after the incorporation of aluminum. The concentration of the Brönsted sites determined from  $^{31}\text{P}$  MAS NMR is about 2 orders of magnitude lower than that of total SiOH groups, which renders their direct observation by  $^1\text{H}$  MAS NMR spectroscopy difficult. However, these sites can be well studied by  $^{31}\text{P} \rightarrow ^1\text{H}$  CP/MAS and various triple-resonance TRAPDOR NMR techniques, which provide a more detailed description of the interactions between TMP and the different hydroxyl groups in the Al–MCM-41 materials. Although the acid strength of the Brönsted sites in the Al–MCM-41 materials is lower than that of microporous zeolites such as HY, these sites can protonate TMP molecules. Some of the framework T-site aluminum atoms are not associated with the bridging hydroxyl groups and are probably present as Al–OH. No Lewis acid sites were found in our samples, though the  $^{27}\text{Al}$  MAS spectra show the existence of five-coordinate extraframework aluminum.

## Introduction

Zeolites with uniform and molecular-size pores have been widely used in industry for a wide range of applications including the adsorption and separation of gases and hydrocarbon, drying, ion exchange, and catalysis.<sup>1</sup> However, they cannot effectively catalyze high molecular weight petroleum fractions because of the limitation of microporous size (usually less than 2 nm). The synthesis of mesoporous silicate materials such as MCM-41<sup>2,3</sup> provides the potential for the materials to function as versatile catalysts and catalyst supports for the conversion of large molecules. MCM-41 (a member of the M41S family), synthesized with surfactant molecules as a structure-directing reagent, possesses a hexagonal arrangement of uniformly sized mesopores with diameters in the range of 1.5–10 nm. The pore sizes can be adjusted by changing the length of the alkyl chains of the surfactant molecules. The resultant mesoporous materials are characterized by long-range periodicity in the arrangements of pores, with locally disordered inorganic frameworks. Since the discovery of MCM-41 by Mobil researchers in 1992, a

number of publications have dealt with its synthesis,<sup>4,5</sup> its sorptive properties,<sup>6,7</sup> its application as a host material for various guest molecules,<sup>8,9</sup> and the nature of isomorphously substituted mesoporous materials.<sup>10,11</sup> Generally, the incorporation of heteroatoms such as Al into the siliceous mesoporous materials will introduce a charge imbalance in the framework that is balanced by protons, thus generating Brönsted acidity on these materials. However, as compared with conventional zeolites, these mesostructured materials have relatively low acidity and hydrothermal stability, which probably limits their practical application in catalytic reactions for the petroleum industry.<sup>12,13</sup> The relatively low acidity of the mesoporous materials may be attributed to the amorphous nature of the pore walls and the special nature of the acid sites. For the application of MCM-41 in catalysis, detailed knowledge concerning the structure of the acid sites in the mesopores of the aluminum-containing materials is desirable. Even though these sites were previously investigated by various spectroscopic techniques<sup>13–20</sup> such as temperature-programmed desorption (TPD), FT-IR, and NMR, their chemical nature is still poorly understood (i.e., if the zeolitelike bridging hydroxyl groups (SiOHAl, Brönsted acid site) are present in these materials and if they can protonate adsorbed molecules). The NMR technique plays an important role in the characterization of the acidity of zeolites and other solid catalysts.<sup>21</sup> However, in previous studies of MCM-

\* To whom correspondence should be addressed. E-mail: dengf@wipm.ac.cn. Fax: +86-27-87199291.

<sup>†</sup> Wuhan Institute of Physics and Mathematics, Chinese Academy of Science.

<sup>‡</sup> Institute of Physics and Center for Condensed Matter Physics, Chinese Academy of Science.

41,<sup>14,19,20</sup> Brönsted acid sites in the MCM-41 materials had never been directly observed by  $^1\text{H}$  NMR spectroscopy and were regarded as “NMR-invisible”.

The acidity of zeolites can be studied using various base probe molecules, namely, pyridine and carbon monoxide.  $\text{NH}_3\text{-TPD}$  is a traditional and probably the most frequently used method for studying the acidity of solid catalysts. Both NMR and IR spectroscopy of adsorbed probe molecules are also extensively employed for this purpose.<sup>22,23</sup> Trimethylphosphine (TMP) was first used in NMR to probe the acidity of the HY zeolite by Lunsford and co-workers<sup>24,25</sup> and has now been widely used to study the acid sites of various zeolites and other solid catalysts.<sup>26–32</sup> TMP is superior to other probe molecules such as acetone and pyridine because of the relatively high NMR sensitivity of  $^{31}\text{P}$ , which is very useful in cases where the concentration of the acid sites is very low or when some double-resonance NMR experiments such as  $^{31}\text{P} \rightarrow ^1\text{H}$  CP/MAS are performed. Furthermore,  $^{31}\text{P}$  NMR has a large chemical-shift range for TMP bound to different acid sites, and Brönsted and Lewis acid sites can be easily distinguished. When Brönsted or Lewis acid sites are present in zeolites, protonated adduct,  $\text{TMPH}^+$ , or Lewis-bound TMP complex are confirmed. The formation of  $\text{TMPH}^+$  will give rise to a  $^{31}\text{P}$  resonance at ca.  $-4$  ppm and a  $J_{\text{P-H}}$  coupling constant of ca. 500 Hz, whereas the Lewis-bound TMP complexes will result in resonances in the shift range from  $-32$  to  $-58$  ppm. Grey et al.<sup>27</sup> recently demonstrated that only the resonance at ca.  $-46$  ppm is due to an aluminum Lewis acid site directly bound to the phosphine molecule. As revealed by Lunsford et al.,<sup>28</sup> the mobility of  $\text{TMPH}^+$  complexes in zeolites mainly depends on the size of the channels, the loading of TMP, and the sample's temperature. Bendada et al.<sup>29</sup> and Grey et al.<sup>30,31</sup> also thoroughly studied the motion of TMP as a function of temperature. More recently, double-resonance NMR and ab initio calculations have been employed to study zeolite HY, which provides a more detailed description of the exact structure of the TMP–Brönsted acid site complex formed in the zeolite.<sup>32</sup>

In this study, we used TMP as a probe molecule to study the nature of acid sites in a series of Al–MCM-41 materials with Si/Al ratios ranging from 16 to 80 by various solid-state NMR techniques including  $^{29}\text{Si}$ ,  $^{31}\text{P}$ ,  $^{27}\text{Al}$ ,  $^1\text{H}$  MAS, and some double- and triple-resonance experiments such as  $^{31}\text{P} \rightarrow ^1\text{H}$  CP/MAS and  $^1\text{H}/^{27}\text{Al}$ ,  $^1\text{H}/^{31}\text{P}/^{27}\text{Al}$  TRAPDOR.

## Experimental Section

**Sample Preparation.** The mesoporous aluminosilicate MCM-41 samples were prepared under mild alkaline conditions using a cetylpyridium chloride (CPCI) surfactant as a templating reagent, as previously described.<sup>33</sup> The composition of the initial aqueous synthesis mixture was, for example (in moles), 1:9.2:0.5:130: $x$  TEOS/ $\text{NH}_4\text{OH}$ /CPCI/ $\text{H}_2\text{O}$ / $\text{Al}(\text{NO}_3)_3$ . The Si/Al ratio was varied from 16 to 80. Tetraethoxysilane (TEOS) was added to a mixture of CPCI, ammonia, and water under stirring, and then  $\text{Al}(\text{NO}_3)_3$  was added to the above-mixed solution under stirring. After the mixture was stirred for more than 30 min, it was loaded into an autoclave and statically heated at 363 K for 72 h. The resultant solid product was recovered by filtration, washing with distilled water, and drying in air. To remove the organic template molecules and get the H-form of the materials, the as-synthesized samples were heated in a thin-bed configuration under flowing air with a rate of  $1\text{ }^\circ\text{C min}^{-1}$  from room temperature to a final temperature of  $540\text{ }^\circ\text{C}$  over a period of 12 h. Pure siliceous MCM-41 material was synthesized in a similar way except that no  $\text{Al}(\text{NO}_3)_3$  was involved. A known

amount of the H-form materials was placed in a glass tube to a bed length of about 10 mm. The tube was connected to a vacuum line. The temperature was gradually increased at a rate of  $1\text{ }^\circ\text{C min}^{-1}$ , and the sample was kept at a final temperature of  $400\text{ }^\circ\text{C}$  at a pressure below  $10^{-3}$  Pa over a period of 12 h and then cooled. After the sample cooled to ambient temperature, a measured volume of TMP with a known pressure was condensed and frozen inside the sample by cooling the sample region of the NMR tube with liquid nitrogen. In some cases, the physisorbed TMP was removed under vacuum at a temperature of ca.  $80\text{ }^\circ\text{C}$  for 0.5 h. Finally, the NMR tube was flame sealed. Prior to making the NMR measurements, the samples were placed into NMR rotors with a Kel-F endcap (cut with 20 grooves)<sup>34</sup> under a dry nitrogen atmosphere in a glovebox.

**NMR Spectroscopy.** All of the NMR experiments were carried out at 9.4 T on a Varian Infinityplus-400 spectrometer using a Chemagnetic triple-resonance 7.5-mm or double-resonance 4-mm probe. The resonance frequencies are 400.12, 161.9, 104.3, and 79.5 MHz for  $^1\text{H}$ ,  $^{31}\text{P}$ ,  $^{27}\text{Al}$ , and  $^{29}\text{Si}$ , respectively. The  $\pi/2$  pulse lengths for  $^1\text{H}$ ,  $^{31}\text{P}$ ,  $^{27}\text{Al}$ , and  $^{29}\text{Si}$  were measured to be 2.0, 4.0, 4.9, and  $4.4\text{ }\mu\text{s}$ , respectively. The excitation pulse lengths were adjusted to  $\pi/4$  for  $^1\text{H}$ ,  $^{29}\text{Si}$ , and  $^{31}\text{P}$  and to  $\pi/12$  for the  $^{27}\text{Al}$  single-pulse experiments. The chemical shifts were referenced to TMS for  $^1\text{H}$  and  $^{29}\text{Si}$ , to a 0.1 M  $\text{Al}(\text{NO}_3)_3$  solution for  $^{27}\text{Al}$ , and to an 85%  $\text{H}_3(\text{PO}_4)$  solution for  $^{31}\text{P}$ . Repetition times of 5, 10, 120, and 0.5 s were used in  $^1\text{H}$ ,  $^{31}\text{P}$ ,  $^{29}\text{Si}$ , and  $^{27}\text{Al}$  NMR experiments, respectively. The MAS spinning speed ranged from 5 to 14 kHz.

**$^1\text{H} \rightarrow ^{31}\text{P}$  and  $^{31}\text{P} \rightarrow ^1\text{H}$  CP.** As suggested by Grey et al.,<sup>32</sup> the Hartmann–Hahn matching condition for  $^{31}\text{P} \leftrightarrow ^1\text{H}$  CP was optimized using  $(\text{NH}_4)_2\text{HPO}_4$ . The contact time for CP was set to be 1 ms. Recycle delays of 2 and 10 s and ca. 5000 and 10 000 scans were used in the  $^1\text{H} \rightarrow ^{31}\text{P}$  and  $^{31}\text{P} \rightarrow ^1\text{H}$  CP experiments for the Al–MCM-41 samples, respectively.

**$^1\text{H}/^{27}\text{Al}/^{31}\text{P}$  TRAPDOR NMR.** Three different kinds of TRAPDOR experiments were performed. The pulse sequences of the first two TRAPDOR experiments are similar to those used in the literature<sup>32,35–40</sup> except that the magnetization of  $^{31}\text{P}$  was prepared via  $^1\text{H} \rightarrow ^{31}\text{P}$  CP in the  $^{31}\text{P}/^{27}\text{Al}$  TRAPDOR experiments, whereas that of  $^1\text{H}$  was obtained via  $^{31}\text{P} \rightarrow ^1\text{H}$  CP in the  $^1\text{H}/^{27}\text{Al}$  TRAPDOR experiments (Figure 1a). The TRAPDOR experiments were carried out with and without  $^{27}\text{Al}$  irradiation during one of the two echo periods,  $\tau$ , which is equal to multiples of the rotor period.<sup>37</sup> The third kind of experiment was performed using the pulse sequence shown in Figure 1b in which  $^1\text{H}$  magnetization is transferred to  $^{31}\text{P}$  via CP after the  $^1\text{H}/^{27}\text{Al}$  TRAPDOR effect is measured. An  $^{27}\text{Al}$  radio-frequency (rf) field amplitude of 62 kHz and a spinning speed of 4 kHz were used for all TRAPDOR NMR experiments.

**$^1\text{H}$ ,  $^{31}\text{P}$ , and  $^{27}\text{Al}$  Spin Counting.** Our  $^1\text{H}$ ,  $^{31}\text{P}$ , and  $^{27}\text{Al}$  spin-counting method was similar to that used in the literature,<sup>32</sup> which was carried out by comparing the integrated intensity of a known amount of an Al–MCM-41 sample with those of adamantane,  $(\text{NH}_4)_2\text{HPO}_4$ , and  $\text{Al}(\text{NO}_3)_3$ , respectively. A small flip-angle (approximately  $15^\circ$ ) pulse was used to record the  $^{27}\text{Al}$  spectra in order to provide a quantitative measurement.<sup>41</sup> For the Al–MCM-41 samples, only the central transition ( $|1/2\rangle \leftrightarrow |-1/2\rangle$ ) was irradiated in the  $^{27}\text{Al}$  spectrum, whereas for aluminum nitrate the outer satellite transitions were also simultaneously irradiated. Massiot et al.<sup>42</sup> have demonstrated that the contribution of the integrated intensity of the outer satellite transitions to the center band of quadrupolar nuclei is determined by the quadrupole frequency ( $\nu_Q$ ) and the spinning speed ( $\nu_r$ ). Using the graphical method of Massiot et al.,<sup>42</sup> we

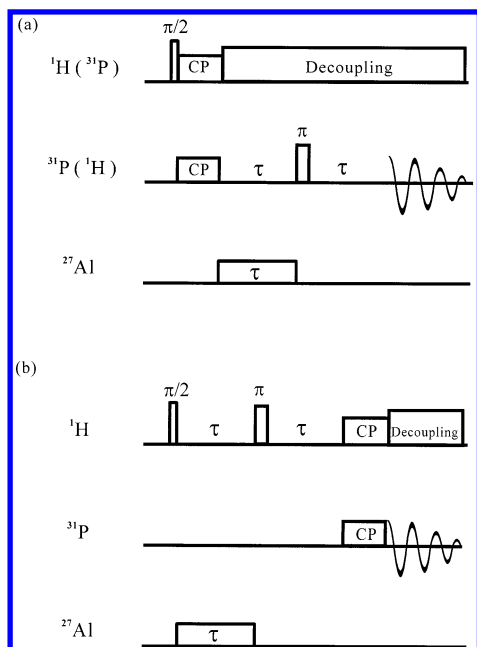


**Figure 1.** Pulse sequences for various triple-resonance experiments: (a)  $^1\text{H}/^{31}\text{P}/^{27}\text{Al}$  or  $^{31}\text{P}/^1\text{H}/^{27}\text{Al}$  CP-TRAPDOR and (b)  $^1\text{H}/^{27}\text{Al}/^{31}\text{P}$  TRAPDOR-CP. See the Experimental Section for more details.

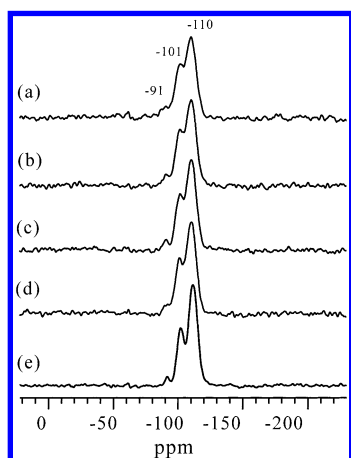


**Figure 2.**  $^{29}\text{Si}$  MAS spectra of Al–MCM-41 materials with various silicon-to-aluminum ratios: (a) 16, (b) 25, (c) 50, (d) 80, and (e)  $\infty$ .

could estimate that this contribution is less than 1% for aluminum nitrate for a spinning speed of 6 kHz, which was used to acquire our  $^{27}\text{Al}$  MAS spectra. (A similar result was obtained by Grey et al.<sup>32</sup>) Therefore, the intensities of the Al–MCM-41 samples can be directly compared with that of the central transition of aluminum nitrate.<sup>32</sup>

## Results and Discussion

**$^{29}\text{Si}$  MAS.** The  $^{29}\text{Si}$  MAS NMR spectra of the template-free Al–MCM-41 materials with different Si/Al ratios are shown in Figure 2. All of the spectra consist of three well-resolved signals at ca.  $-90$ ,  $-101$ , and  $-109$  ppm, which can be assigned to  $\text{Q}^2$ ,  $\text{Q}^3$ , and  $\text{Q}^4$  ( $\text{Si}(\text{OSi})_4$ ) sites, respectively. This assignment is also in agreement with the typical shift ranges established from a large number of data measured for various types of zeolites and other silicates.  $n$  of  $\text{Q}^n$  ( $n = 0-4$ ) represents the number of neighboring silicon atoms that are connected with an oxygen bridge. For the Al–MCM-41 sample, the  $\text{Q}^2$  sites probably results from a combination of  $\text{Si}(\text{OSi})_2(\text{OAl})_2$ ,  $\text{Si}(\text{OSi})_2(\text{OAl})(\text{OH})$ , and  $\text{Si}(\text{OSi})_2(\text{OH})_2$ , whereas the  $\text{Q}^3$  sites probably results from both the  $\text{Si}(\text{OSi})_3(\text{OAl})$  and  $\text{Si}(\text{OSi})_3(\text{OH})$  structural units.

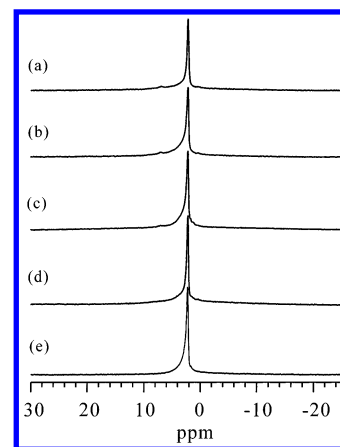


**Figure 3.**  $^1\text{H}$  MAS spectra of Al–MCM-41 materials with various silicon-to-aluminum ratios: (a) 16, (b) 25, (c) 50, (d) 80, and (e)  $\infty$ .

Compared with pure siliceous MCM-41 material, the incorporation of aluminum into the framework causes a slight low-field shift (ca. 1–1.5 ppm) for each site, including the  $\text{Q}^4$  sites that are not associated with aluminum, and as expected, although not significantly, the line widths of each site of the aluminum-containing samples are slightly broadened, probably because of the incorporation of Al into the framework. It is important that the incorporation of aluminum did not lead to an increase in the concentration of the  $\text{Q}^3$  sites or to a simultaneous decrease in the concentration of  $\text{Q}^4$  sites as it does in microporous zeolites, corresponding to a transformation from  $\text{Si}(\text{OSi})_4$  to  $\text{Si}(\text{OSi})_3(\text{OAl})$ . Therefore, the  $\text{Q}^3$  sites should mainly arise from the  $\text{Si}(\text{OSi})_3(\text{OH})$  rather than the  $\text{Si}(\text{OSi})_3(\text{OAl})$  structural units.

**$^1\text{H}$  MAS and  $^1\text{H}/^{27}\text{Al}$  TRAPDOR NMR.** The  $^1\text{H}$  MAS NMR spectra (Figure 3) of the series of Al–MCM-41 samples are very similar to those reported by Hunger et al.<sup>14,15</sup> Signals are present in the chemical shift range of 2.2–3.4 ppm, which can be attributed to silanol groups in inorganic solids. The asymmetric line shape of these signals is likely due to the presence of different types of silanol groups such as isolated and geminal  $\text{SiOH}$  groups and the internal silanol groups.<sup>14</sup> However, at present, we cannot rule out the possibility that part of the shoulder peak in the low-field region originates from the hydroxyl groups associated with aluminum. As revealed by FT-IR, the concentration of Brönsted sites in aluminum-containing MCM-41 samples was about 2 orders of magnitude lower than the concentration of weakly acidic silanol groups, which would make their direct observation by FT-IR or  $^1\text{H}$  MAS NMR difficult. To establish the correlation between the various hydroxyl groups and Al, we performed  $^1\text{H}/^{27}\text{Al}$  TRAPDOR experiments on the Al–MCM-41 samples. These experiments are analogous to dipolar dephasing experiments. Under  $^{27}\text{Al}$  irradiation, the signals of protons that are strongly coupled to aluminum atoms will be significantly suppressed, whereas those that are not coupled with aluminum atoms will remain unaffected. Hence, it is a measure of the heteronuclear dipolar interaction between spins. Figure 4 outlines a typical TRAPDOR result for the Al–MCM-41 sample with Si/Al = 16. A low spinning speed (4.0 kHz) was used to enhance the TRAPDOR effect. On-resonance  $^{27}\text{Al}$  irradiation for two rotor periods (500  $\mu\text{s}$ ) may cause a slight decrease in the signals, and two weak resonances at 1.9 and 3.5 ppm remain in the difference spectrum (see Figure 4c), indicating that they are associated with hydroxyl groups in close proximity to aluminum. The 7.0 ppm signal shows a negligible TRAPDOR effect and can be attributed to the residual ammonium ions. The weak TRAPDOR effects for the signals at 1.9 and 3.5 ppm may result partially from the

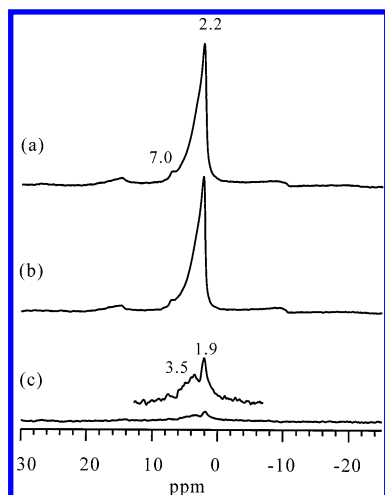


**Figure 4.**  $^1\text{H}/^{27}\text{Al}$  TRAPDOR spectra of Al-MCM-41 material with Si/Al = 16 (a) without  $^{27}\text{Al}$  irradiation (the control experiment), (b) with  $^{27}\text{Al}$  irradiation, and (c) difference spectrum a - b (spinning speed = 4 kHz and  $^{27}\text{Al}$  irradiation time = 250  $\mu\text{s}$  corresponding to one rotor period.)

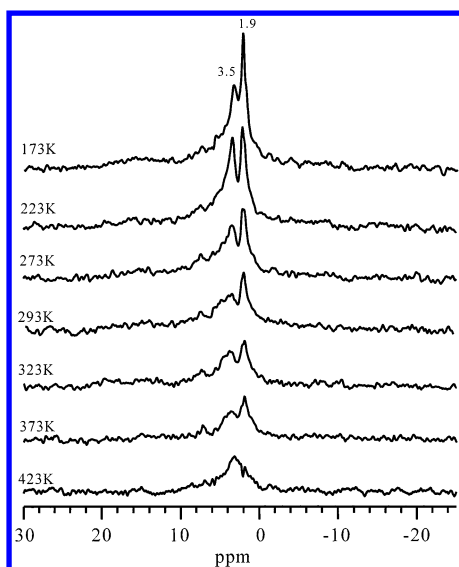


**Figure 5.**  $^1\text{H}/^{27}\text{Al}$  TRAPDOR difference spectra of Al-MCM-41 with Si/Al = 16 as a function of temperature (drawn in an absolute intensity mode).

low concentration of these hydroxyl groups and partially from their high mobility at ambient temperature, which will reduce the heteronuclear  $^1\text{H}$ - $^{27}\text{Al}$  dipolar interaction. We also performed variable-temperature (VT)  $^1\text{H}/^{27}\text{Al}$  TRAPDOR experiments on the Al-MCM-41 sample with Si/Al = 16. It can be seen from the VT difference TRAPDOR spectra (Figure 5) that the lower the temperature the stronger the TRAPDOR effects for the signals at 1.9 and 3.5 ppm. Since only the protons coupled to aluminum atoms will survive in the difference spectrum, the  $^1\text{H}/^{27}\text{Al}$  TRAPDOR experiments strongly demonstrate that at least some of the signals in the  $^1\text{H}$  MAS spectra are associated with hydroxyl groups that are coupled to aluminum. Their relative concentrations cannot be determined from the  $^1\text{H}/^{27}\text{Al}$  TRAPDOR spectra because of the variation in dipolar dephasing efficiencies for nuclei as a function of the chemical and motional environments. According to their chemical shifts, we tentatively assign the 1.9 ppm signal to the aluminum hydroxyl group and the 3.5 ppm signal to the bridging hydroxyl groups (SiOHAl). This assignment is quite different from that of Hunger et al.<sup>15</sup> They observed a weak signal at 2.6 ppm and

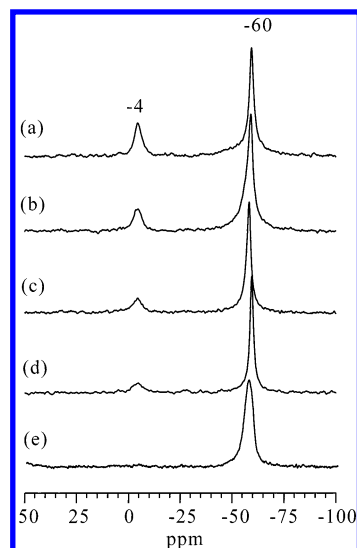


**Figure 6.**  $^{31}\text{P}$  MAS spectra of TMP adsorbed on Al-MCM-41 materials with various silicon-to-aluminum ratios: (a) 16, (b) 25, (c) 50, (d) 80, and (e)  $\infty$ . The spectra were recorded with  $^1\text{H}$  decoupling.

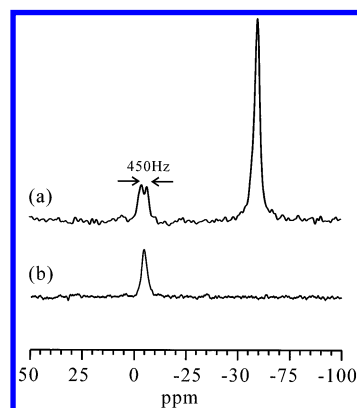


**Figure 7.**  $^{31}\text{P}$  MAS spectra of TMP adsorbed on Al-MCM-41 with Si/Al = 16 recorded under different conditions: (a) without degassing and  $^1\text{H}$  decoupling ( $^{31}\text{P}$ - $^1\text{H}$  coupling constant  $J$  is about 450 Hz) and (b) degassed at 80  $^\circ\text{C}$  for 0.5 h with  $^1\text{H}$  decoupling.

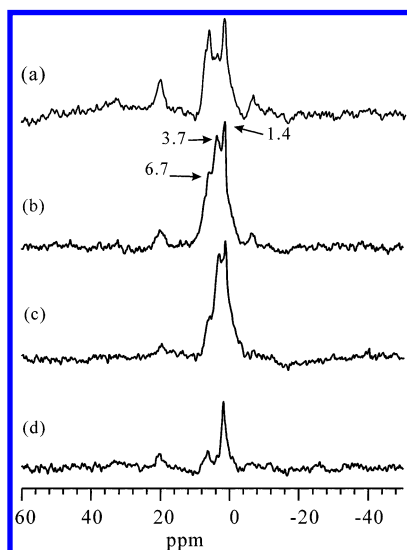
a strong signal at 1.8 ppm in the  $^1\text{H}/^{27}\text{Al}$  TRAPDOR difference spectrum of an Al-MCM-41 sample (Si/Al = 15) and ascribed the former to AlOH groups and the latter to SiOH in the vicinity of aluminum atoms, a structure similar to that of bridging hydroxyl groups. However, it is difficult to understand why such a structural model would result in two separate  $^1\text{H}$  resonances.

**$^{31}\text{P}$  MAS and  $^{31}\text{P} \rightarrow ^1\text{H}$  CP/MAS.** The  $^{31}\text{P}$  MAS NMR spectra (Figure 6) of TMP adsorbed on the series of Al-MCM-41 samples consist of two resonances at -4 and -59 ppm. We found that the latter could be completely removed but the former remains almost unchanged (Figure 7b) by degassing the corresponding sample at 80  $^\circ\text{C}$  for 0.5 h on a vacuum line, suggesting that the -59 ppm signal is likely due to the physisorbed or weakly bound TMP. The signal at -4 ppm falls within the chemical-shift range of TMP adsorbed on Brönsted acid sites.<sup>25,32</sup> However, at this time, we cannot give an unambiguous assignment for the -4 ppm resonance because of the large difference in the topological structure between the mesoporous materials and microporous molecular sieves. For pure siliceous MCM-41, only the resonance at -59 ppm is present (Figure 6e). A similar phenomenon was observed for TMP adsorbed on  $\gamma$ -alumina, where various types of aluminum hydroxyl groups are present.<sup>25</sup> Thus, the -4 ppm signal is not associated with TMP adsorbed on either silanol or aluminum



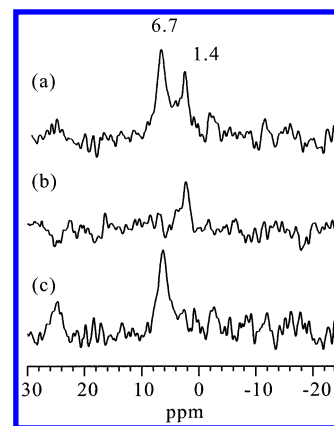
**TABLE 1: Concentrations of Hydroxyl Groups and Framework T-Site Aluminum in Al-MCM-41 Materials**

Si/Al	Brönsted acid sites (mmol/g)	total OH groups (mmol/g)	T-site aluminum (mmol/g)
16	$8.9 \times 10^{-2}$	3.6	$3.3 \times 10^{-1}$
25	$5.7 \times 10^{-2}$	3.4	$2.0 \times 10^{-1}$
50	$4.4 \times 10^{-2}$	4.0	$1.3 \times 10^{-1}$
80	$3.4 \times 10^{-2}$	4.1	$7.8 \times 10^{-2}$

**Figure 8.**  $^{31}\text{P} \rightarrow ^1\text{H}$  CP/MAS spectra of TMP adsorbed on Al–MCM-41 materials with various silicon-to-aluminum ratios: (a) 16, (b) 25, (c) 50, and (d) 80.

hydroxyl groups and is most likely due to TMP adsorbed on the bridging hydroxyl groups (SiOHAl). The intensity of the  $-4$  ppm signal increases gradually with the increase in the Al concentration in the MCM-41 materials (decreasing the Si/Al ratios), implying an increase in the concentration of the Brönsted acid sites. The concentrations of the Brönsted acid sites for the series of Al–MCM-41 materials can be quantitatively obtained from the corresponding  $^{31}\text{P}$  MAS spectra, and the results are listed in Table 1. In the absence of proton decoupling during the acquisition period, the peak at  $-4$  ppm splits into a doublet because of  $^{31}\text{P}$ – $^1\text{H}$   $J$  coupling, which can clearly be observed when the spinning speed is greater than 10 kHz (Figure 7a). The coupling constant  $J$  is about 450 Hz, which is slightly smaller than that in zeolite HZSM-5 (480 Hz).<sup>28</sup>

The  $^{31}\text{P} \rightarrow ^1\text{H}$  CP/MAS experiments were performed to select the signal of the proton associated with TMP. Three peaks can be well resolved at ca. 6.7, 3.7, and 1.4 ppm in the  $^{31}\text{P} \rightarrow ^1\text{H}$  CP/MAS spectra of the series of TMP/Al–MCM-41 samples (Figure 8). Grey et al.<sup>32</sup> observed two resonances at 7.8 and 1.5 ppm in the  $^{31}\text{P} \rightarrow ^1\text{H}$  CP MAS spectrum of a TMP/HY sample and ascribed them to protons (of the Brönsted acid site) directly attached to the phosphorus atoms and the three methyl groups of  $\text{TMPH}^+$ , respectively. A similar assignment can be made for the 6.7 and 1.4 ppm resonances observed in our  $^{31}\text{P} \rightarrow ^1\text{H}$  CP/MAS spectra. The intensity of the resonance at 6.7 ppm grows with the increase in Al content, which is in line with the  $^{31}\text{P}$  MAS result. We found that the intensity of the 3.4 ppm signal was largely reduced after the corresponding samples were evacuated at 80 °C for 1 h. Hence, we tentatively ascribe this signal to the weakly acidic silanol groups bound to TMP. To give more detailed information about the nature of the TMP complexes formed in the mesoporous Al–MCM-41 materials, we applied  $^{31}\text{P}/^1\text{H}/^{27}\text{Al}$  (or  $^1\text{H}/^{31}\text{P}/^{27}\text{Al}$ ) CP-TRAPDOR and  $^1\text{H}/^{27}\text{Al}/^{31}\text{P}$  TRAPDOR-CP experiments to these samples.

**Figure 9.**  $^{31}\text{P}/^1\text{H}/^{27}\text{Al}$  CP-TRAPDOR spectra of TMP adsorbed on Al–MCM-41 with Si/Al = 16 (a) without  $^{27}\text{Al}$  irradiation (the control experiment), (b) with  $^{27}\text{Al}$  irradiation, and (c) difference spectrum a – b.  $^1\text{H}$  magnetization was prepared via the  $^{31}\text{P} \rightarrow ^1\text{H}$  CP experiment to select the protons near TMP, and then the TRAPDOR effect between  $^1\text{H}$  and  $^{27}\text{Al}$  was measured (spinning speed = 4 kHz and  $^{27}\text{Al}$  irradiation time = 750  $\mu\text{s}$  corresponding to three rotor periods).

**$^{31}\text{P}/^1\text{H}/^{27}\text{Al}$  ( $^1\text{H}/^{31}\text{P}/^{27}\text{Al}$ ) CP-TRAPDOR and  $^1\text{H}/^{27}\text{Al}/^{31}\text{P}$  TRAPDOR-CP.** Figure 9 shows a representative  $^{31}\text{P}/^1\text{H}/^{27}\text{Al}$  CP-TRAPDOR spectra of the TMP/Al–MCM-41 sample (Si/Al = 16, degassing at 80 °C for 0.5 h) using the pulse sequence shown in Figure 1a. Proton magnetization was prepared via  $^{31}\text{P} \rightarrow ^1\text{H}$  cross polarization, and then the TRAPDOR effect between  $^1\text{H}$  and  $^{27}\text{Al}$  was measured. The experiment establishes a  $^{31}\text{P} \rightarrow ^1\text{H} \rightarrow ^{27}\text{Al}$  correlation pathway. Since the echo time was set to three rotor periods (750  $\mu\text{s}$ ) to enhance the TRAPDOR effect, relatively weak signals were acquired in this case (because of the spin–spin relaxation effect). Two major peaks at 1.4 and 6.7 ppm are present in the control experiment (without  $^{27}\text{Al}$  irradiation). Under  $^{27}\text{Al}$  irradiation, the 6.7 ppm peak is almost completely suppressed. This strongly supports the above assignment that this signal originates from protons (of the Brönsted acid site) directly attached to the phosphorus atoms of  $\text{TMPH}^+$ . That is to say, the zeolite-like bridging hydroxyl groups (SiOHAl, Brönsted acid site) have really formed after the incorporation of Al into the MCM-41 materials. Although a lower signal-to-noise ratio is achieved, it can be expected that the 1.4 ppm signal will show a negligible TRAPDOR effect, which is likely due to the relatively large distance between the protons of the three methyl groups of  $\text{TMPH}^+$  and the framework Brönsted site Al.

We also performed a  $^1\text{H}/^{31}\text{P}/^{27}\text{Al}$  CP-TRAPDOR experiment on the TMP/Al–MCM-41 sample (Si/Al = 16) in which  $^{31}\text{P}$  magnetization was established via  $^1\text{H} \rightarrow ^{31}\text{P}$  CP and then the TRAPDOR effect between  $^{31}\text{P}$  and  $^{27}\text{Al}$  was measured. This experiment provides the  $^1\text{H} \rightarrow ^{31}\text{P} \rightarrow ^{27}\text{Al}$  proximity. We could not observe the  $^{31}\text{P}/^{27}\text{Al}$  TRAPDOR effect at ambient temperature. Even though we had to lower the temperature to  $-150$  °C, the TRAPDOR effect is still very weak (Figure 10). This is partially due to the relatively large distance between  $^{31}\text{P}$  and  $^{27}\text{Al}$  and partially to the motion of the  $\text{TMPH}^+$  complex even at temperature as low as  $-150$  °C. It can be expected that the molecular motion of the  $\text{TMPH}^+$  complex will be much less restricted in the mesoporous materials than in the microporous molecular sieves, where a very strong  $^{31}\text{P}/^{27}\text{Al}$  TRAPDOR effect was observed at  $-150$  °C for a TMP/HY sample.

Since the  $^{31}\text{P}$  spin–lattice relaxation time of the  $\text{TMPH}^+$  complex is ca. 2 s and cross polarization from  $^{31}\text{P}$  to  $^1\text{H}$  ( $\propto \gamma_{\text{P}}/\gamma_{\text{H}} \approx 0.4$ ) is much less efficient than that from  $^1\text{H}$  to  $^{31}\text{P}$  ( $\propto \gamma_{\text{H}}/\gamma_{\text{P}} \approx 2.5$ ), the  $^{31}\text{P}/^1\text{H}/^{27}\text{Al}$  CP-TRAPDOR experiment

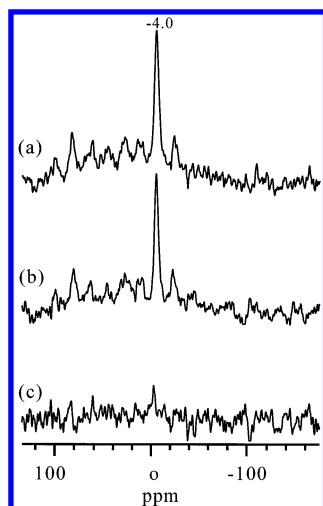


**Figure 10.**  $^1\text{H}/^{31}\text{P}/^{27}\text{Al}$  CP-TRAPDOR spectra of TMP adsorbed on Al-MCM-41 with Si/Al = 16 recorded at  $-150^\circ\text{C}$  (a) without  $^{27}\text{Al}$  irradiation (the control experiment), (b) with  $^{27}\text{Al}$  irradiation, and (c) difference spectrum  $a - b$ .  $^{31}\text{P}$  magnetization was prepared via the  $^1\text{H} \rightarrow ^{31}\text{P}$  CP experiment, and then the TRAPDOR effect between  $^{31}\text{P}$  and  $^{27}\text{Al}$  was measured (spinning speed = 4 kHz and  $^{27}\text{Al}$  irradiation time = 250  $\mu\text{s}$ ).

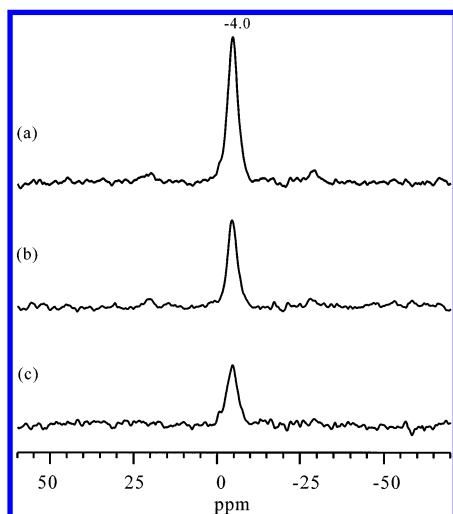


**Figure 11.**  $^1\text{H}/^{27}\text{Al}/^{31}\text{P}$  TRAPDOR-CP spectra of TMP adsorbed on Al-MCM-41 with Si/Al = 16 (a) without  $^{27}\text{Al}$  irradiation (the control experiment), (b) with  $^{27}\text{Al}$  irradiation, and (c) difference spectrum  $a - b$ .  $^1\text{H}$  magnetization is transferred to  $^{31}\text{P}$  via  $^1\text{H} \rightarrow ^{31}\text{P}$  CP after the  $^1\text{H}/^{27}\text{Al}$  TRAPDOR effect is measured.

is very time-consuming and gives rise to a low signal-to-noise ratio. (See Figure 9.) We proposed a new pulse sequence (Figure 1b) with which to perform  $^1\text{H}/^{27}\text{Al}/^{31}\text{P}$  TRAPDOR-CP experiments in which the  $^1\text{H}/^{27}\text{Al}$  TRAPDOR effect is first measured and then  $^1\text{H}$  magnetization is transferred to  $^{31}\text{P}$  via CP for acquisition. This experiment establishes the  $^{27}\text{Al} \rightarrow ^1\text{H} \rightarrow ^{31}\text{P}$  correlation. Figure 11 shows the  $^1\text{H}/^{27}\text{Al}/^{31}\text{P}$  TRAPDOR-CP spectra of the TMP/Al-MCM-41 sample (Si/Al = 16). Apparently, a strong  $^1\text{H}/^{27}\text{Al}$  TRAPDOR effect was observed for the resonance at  $-4$  ppm. The experiment demonstrates that the phosphorus atom giving rise to the resonance at  $-4$  ppm should be in close proximity to a proton that is also associated with an aluminum atom. Therefore, the  $-4$  ppm signal in the  $^{31}\text{P}$  MAS NMR spectra can be unambiguously assigned to the  $\text{TMPH}^+$ /Brönsted sites complex formed in the Al-MCM-41 materials.

**$^{27}\text{Al}$  MAS NMR.** The  $^{27}\text{Al}$  MAS NMR spectra (not shown) of the parent materials consists of only one resonance at 54 ppm due to four-coordinate framework aluminum, indicating

that most of the aluminum atoms are incorporated into the framework of the Al-MCM-41 materials. However, the  $^{27}\text{Al}$  MAS NMR spectra (Figure 12, left) of the calcined and rehydrated Al-MCM-41 materials show an intense resonance at 54 ppm and two other small signals at 30 and 0 ppm, which are probably caused by five- and six-coordinate aluminum atoms at extra-framework positions that are generated during the calcination process. Since the walls of mesoporous MCM-41 consist of a locally disordered inorganic framework, “framework” Al also refers to Al that is located in the walls of the materials whereas “extraframework Al” refers to Al that is located outside the walls. The intensity of the 54 ppm signal increases with the aluminum content of the samples, which is consistent with  $^{31}\text{P}$  NMR results. Recent studies have shown that some of the octahedral aluminums can be present in the framework of some microporous zeolites (such as HY, HZSM-5, and zeolite beta) in the presence of water molecules and can be converted into tetrahedral aluminum by the adsorption of ammonia.<sup>14,43,44</sup> As pointed out by Wouters et al.,<sup>44</sup> a partial hydrolysis of framework Al-O bonds generates framework-connected Al-OH species that can host two water molecules, giving rise to octahedral aluminum species. The subsequent adsorption of ammonia will convert this octahedral aluminum back to tetrahedral Al. However, the detailed mechanism for the octahedral-to-tetrahedral conversion is not well understood. We also used ammonia to check the bonding state of octahedral aluminum in our Al-MCM-41 samples. After the adsorption of ammonia, the 0 ppm signal disappears, but the 30 ppm signal remains almost unchanged (Figure 12, right), suggesting that the former is associated with four-coordinate framework aluminum and the latter results from extra-framework aluminum. The concentrations of the four-coordinate (T-site) framework aluminum atoms were determined from the corresponding  $^{27}\text{Al}$  MAS spectra and are listed in Table 1.

**Acidity of the Al-MCM-41 Materials.** Generally, the chemical shift of the hydroxyl groups increases with increasing acidity if hydrogen bonding is absent. The correlation between the chemical shift and the acidity was well established for all types of surface hydroxyl groups of zeolites and other oxide catalysts by  $^1\text{H}$  MAS NMR as well as quantum chemical calculations.<sup>45,46</sup> The  $^1\text{H}$  chemical shift (ca. 3.5 ppm) of Brönsted acid sites observed for the Al-MCM-41 materials is smaller than that of zeolites (ca. 4.3 ppm for HZSM-5). Thus, it can be expected that the acidity of the Al-MCM-41 samples should be weaker than that of microporous zeolites. The experimental  $^{31}\text{P}$  chemical shift (of  $-4$  ppm) is very close to those observed previously for microporous zeolites where there is nearly a complete transfer of the proton from the zeolite lattice to TMP, indicating that the  $\text{TMPH}^+$  complex is formed in the Al-MCM-41 samples. The relatively small  $^{31}\text{P}-^1\text{H}$   $J$  coupling constant (of ca. 450 Hz) as compared with those observed for microporous zeolites (480–520 Hz) also indicates that the acid strength of the Al-MCM-41 material is lower than that of zeolites. Since the scalar  $J$  coupling operates through “bonds” (i.e., by orbital overlap), bonding connectivities between the phosphorus atom of TMP and the protons of Brönsted sites are obtained unambiguously. In addition, our various TRAPDOR experiments also strongly support the formation of the  $\text{TMPH}^+$ /Brönsted sites complex in the Al-MCM-41 samples. Hunger et al.<sup>14</sup> used deuterated pyridine to study the acid strength of Al-MCM-41 materials and found that the interaction between pyridine molecules and silanol groups resulted in the formation of hydrogen-bonded adsorbate complexes and shifted the resonance position of SiOH groups from 1.8 to ca. 9.5 ppm.

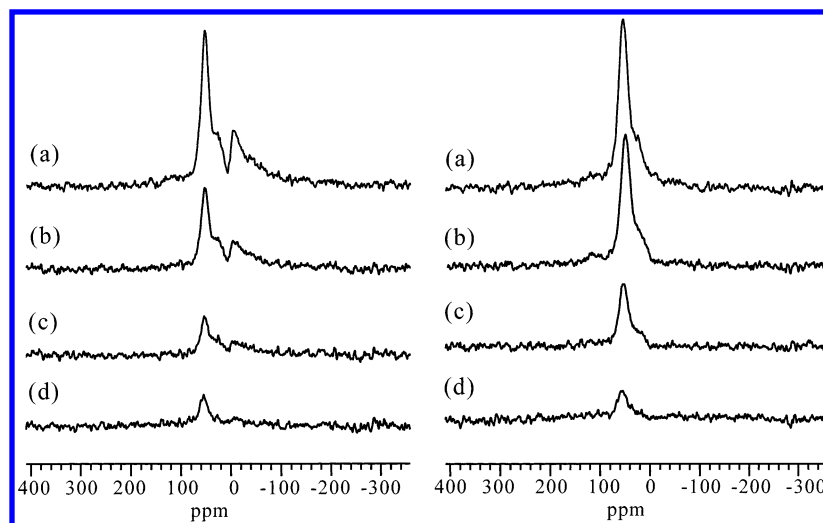


**Figure 12.**  $^{27}\text{Al}$  MAS spectra of Al-MCM-41 materials with various silicon-to-aluminum ratios ((a) 16, (b) 25, (c) 50, and (d) 80) recorded in the calcined and hydrated states (left) and after the subsequent adsorption of ammonia (right).

However, they could not determine the acid strength of Brönsted sites because of their low concentration.

The concentration of Brönsted acid sites ( $\sim 10^{-3}$  mmol/g) in Al-MCM-41 determined by  $^{31}\text{P}$  NMR is about 2 orders of magnitude lower than that of the SiOH groups, which is in line with the previous IR experimental measurements. This may be the reason that they are usually “invisible” in the  $^1\text{H}$  MAS spectra. As shown above, these sites could be easily probed by  $^{31}\text{P}$  NMR of TMP, and their signals could be selectively enhanced or suppressed (or decreased) by  $^{31}\text{P} \rightarrow ^1\text{H}$  CP/MAS and various TRAPDOR experiments. In recent studies,<sup>14,15</sup> ammonia was used to detect Brönsted acid sites in Al-MCM-41 (with Si/Al = 20) by measuring the  $^1\text{H}$  NMR signal (at 7 ppm) of ammonium ions, and their concentration ( $1.8 \times 10^{-2}$  mmol/g) was found to be only about 1 order of magnitude lower than that of the whole concentration of silanol groups ( $2.6 \times 10^{-1}$  mmol/g). One possibility for this discrepancy is that ammonia is a strong base and it can interact with both the Brönsted acid sites and some of the weakly acidic silanol groups to form ammonium ions. However, in the  $^{31}\text{P}$  MAS spectrum of TMP adsorbed on pure siliceous MCM-41, we observe only the signal of physisorbed or weakly bound TMP (at -59 ppm), indicating that no Brönsted acid sites are present in this sample and that the complex formed between TMP and weakly acidic silanol groups should give no contribution to the  $^{31}\text{P}$  signal of Brönsted acid sites at -4 ppm. Thus, we believe that  $^{31}\text{P}$  MAS NMR provides a more accurate determination of the concentration of Brönsted acid sites than  $^1\text{H}$  MAS NMR.

It is generally accepted that one framework tetrahedral (T-site) aluminum corresponds to one Brönsted acid site in microporous zeolites. Recently, Grey et al.<sup>32,47</sup> indicated that the  $^{15}\text{N}$ /visible T-site  $^{27}\text{Al}$  ratio was close to 1:1 for the MMA (monomethylamine)/HY system whereas the  $^{31}\text{P}$ /visible T-site  $^{27}\text{Al}$  ratio varied from 1:1.7 to 1:1.3 for the TMP/HY system, implying that some of the aluminum T-sites that were not directly bound to TMP were visible in the latter case when using the  $^{27}\text{Al}$  MAS method. This is likely due to the relatively large TMP molecule, in comparison with MMA, making some of the aluminum T-sites, especially those in the small sodalite cages, inaccessible. In the present case, the measured values (Table 1) of 1:2.3 to 1:3.7 for the  $^{31}\text{P}$ /visible T-site  $^{27}\text{Al}$  ratio suggest that about 56 to 73% of the total T-site aluminum atoms are not associated with the bridging hydroxyl groups (Brönsted acid sites) for the Al-MCM-41 materials with different Si/Al ratios

if all of the T-sites are accessible to TMP. Hunger et al.<sup>14</sup> also concluded that the concentration of Brönsted acid sites amounts to only one-fourth of the total number of Al species for an Al-MCM-41 sample with Si/Al = 20. However, they did not give a detailed description of the local structure of the aluminum sites. In principle, the negative charge on these T-site aluminum atoms (not associated with Brönsted sites) should be balanced by protons, forming AlOH groups.

The  $^1\text{H}$  chemical shifts of the different AlOH groups vary over a wide range, depending on their specific structure in the different materials. In amorphous  $\gamma$ -alumina, there are three types of OH groups:<sup>48</sup> a terminal OH group attached to a single tetrahedral or octahedral Al ( $\text{OHAl}_\text{O}$  or  $\text{OHAl}_\text{T}$ ), a bridging OH coordinated to two octahedral Al ( $\text{OH}_2\text{Al}_\text{O}$ ) or to one tetrahedral Al and one octahedral Al ( $\text{OHAl}_\text{OAl}_\text{T}$ ), and a bridging OH attached to three octahedral Al ( $\text{OH}_3\text{Al}_\text{O}$ ), giving rise to  $^1\text{H}$  signals at ca. 0, 2.5, and 4.3 ppm, respectively.<sup>49,50</sup> However, for a high-surface-area alumina (pseudoboehmite), Fitzgerald et al.<sup>51</sup>, using the CRAMPS technique, observed two peaks at ca. 3.0 and 8.2 ppm that were attributed to ( $\text{OHAl}_\text{O}$ ) and ( $\text{OH}_2\text{Al}_\text{O}$ ), respectively. In a microporous zeolite, the hydroxyl groups associated with framework or extraframework Al give rise to a  $^1\text{H}$  signal at ca. 3.0 ppm. Although our VT  $^1\text{H}/^{27}\text{Al}$  TRAPDOR experiments indicate that the 1.9 ppm peak in the  $^1\text{H}$  spectra is associated with the hydroxyl group bound to aluminum, we are unable to determine whether it is a terminal or bridging aluminum OH group. Further experiments, especially the  $^{17}\text{O}$  multiple quantum magic-angle spinning (MQMAS) technique that can unambiguously discriminate between  $^{17}\text{O}$  signals from Al-O-Si, Si-O-Si, and Al-O-Al linkages,<sup>52-54</sup> may be helpful in clarifying whether the bridging aluminum OH group is really present in the Al-MCM-41 materials. In combination with our  $^{27}\text{Al}$  MAS results, we tentatively ascribe the 1.9 ppm signal to the framework-connected tetrahedral AlOH group.

It is well known that TMP bound to Lewis acid sites of zeolites gives rise to resonances in the chemical-shift range from -32 to -58 ppm. Recently, Grey et al.<sup>26</sup> demonstrated that only the resonance at approximately -46 ppm corresponds to an aluminum Lewis acid site directly bound to the phosphine molecule in dehydroxylated HY. However, in the present case, only the physisorbed or weakly bound TMP was detected by  $^{31}\text{P}$  NMR, giving rise to the -59 ppm resonance that can be easily removed by degassing the corresponding sample at 80 °C. We therefore believe that the Lewis acid site is either absent



or present at a concentration that is below the detection limit of our Al–MCM-41 materials. This finding is quite different from the IR experiment of pyridine adsorbed on Al–MCM-41, which indicates the existence of strong Lewis acid sites with a concentration that is 2–3 times higher than that of Brönsted acid sites. We ascribe part of this discrepancy to the different synthesis method rather than to the inaccessibility of the Lewis acid sites by TMP molecules because the pore size of MCM-41 is much larger than the molecular size of TMP. For microporous zeolites, tricoordinate framework aluminum atoms or extraframework aluminum species are generally regarded as the source of Lewis acidity. Although five-coordinate extraframework aluminum sites are observed in the  $^{27}\text{Al}$  MAS spectra, these sites actually do not act as Lewis centers in the Al–MCM-41 materials, as revealed by  $^{31}\text{P}$  MAS NMR.

## Conclusions

NMR results shows that zeolitelike Brönsted acid sites (SiOHAl) have been formed in the Al–MCM-41 materials and that the concentration of these sites is about 2 orders of magnitude lower than that of the total silanol groups, which usually makes them invisible in the  $^1\text{H}$  MAS spectrum.  $^{31}\text{P}$  MAS NMR suggests that the  $\text{TMPH}^+$  complex, which is characterized by a  $^{31}\text{P}$  chemical shift of  $-4$  ppm and a  $^{31}\text{P}$ – $^1\text{H}$   $J$  coupling of 450 Hz, is formed between adsorbed TMP and the Brönsted acid sites.  $^{31}\text{P} \rightarrow ^1\text{H}$  CP/MAS and various triple-resonance TRAPDOR NMR experiments also strongly support the above assignment and provide a more detailed description of the interactions between TMP and the different hydroxyl groups in the Al–MCM-41 materials. The acid strength of the materials is lower than that of zeolites such as HY and HZM-5. Some of the framework T-site aluminum atoms are not associated with the bridging hydroxyl groups (SiOHAl) and are likely to be present as a tetrahedral AlOH group, giving rise to the  $^1\text{H}$  resonance at 1.9 ppm. It is interesting that no Lewis acid sites were detected by  $^{31}\text{P}$  NMR, though  $^{27}\text{Al}$  MAS NMR shows the existence of extraframework aluminum, which is likely due to the low concentration of these sites formed in the materials. This study shows that the various double- or triple-resonance experiments are powerful tools for establishing correlations between the adsorbate and the surface of mesoporous materials.

**Acknowledgment.** We are grateful to the National Science Foundation of China (grants 29973058 and 20173072) for financial support.

**Note Added after ASAP Posting.** This paper was posted ASAP on 11/19/2002. The authors modified the text of the manuscript in the Introduction and Experimental Section to remove language that was too similar to that of published manuscripts. The corrected version was posted 2/21/2003.

## References and Notes

- Hölderich, W. F.; van Bekkum, H. *Stud. Surf. Sci. Catal.* **1991**, 58, 631.
- Kresge, C. T.; Leonowicz, M. E.; Roth, W. J.; Vartulli, J. C.; Beck, J. S. *Nature (London)* **1992**, 359, 710.
- Beck, J. S.; Vartulli, J. C.; Roth, W. J.; Leonowicz, M. E.; Kresge, C. T.; Schmitt, K. D.; Chu, C. T. W.; Olson, D. H.; Sheppard, E. W.; McCullen, S. B.; Higgins, J. B.; Schlenker, J. L. *J. Am. Chem. Soc.* **1992**, 114, 10834.
- Chen, C. Y.; Burkett, S. L.; Li, H. X.; Davis, M. E. *Microporous Mater.* **1993**, 2, 27.
- Vartulli, J. C.; Schmitt, K. D.; Kresge, C. T.; Roth, W. J.; Leonowicz, M. E.; McCullen, S. B.; Hellring, S. D.; Beck, J. S.; Schlenker, J. L.; Olson, D. H.; Sheppard, E. W. *Stud. Surf. Sci. Catal.* **1994**, 84, 53.
- Rathousky, J.; Zukal, A.; Franke, O.; Schulz-Ekloff, G. *J. Chem. Soc., Faraday Trans.* **1995**, 91, 937.
- Boger, T.; Roesky, R.; Gläser, R.; Ernst, S.; Eigenberger, G.; Weitkamp, J. *Microporous Mater.* **1997**, 8, 79.
- Kozhevnikov, I. V.; Sinnema, A.; Jansen, R. J. J.; Pamin, K.; van Bekkum, H. *Catal. Lett.* **1995**, 30, 241.
- Ernst, S.; Gläser, R.; Selle, M. *Stud. Surf. Sci. Catal.* **1997**, 105, 1021.
- Luan, Z. H.; Cheng, C. F.; He, H. Y.; Klinowski, J. *J. Phys. Chem.* **1995**, 99, 10590.
- Trong, O. D.; Joshi, P. N.; Kaliaguine, S. *J. Phys. Chem.* **1996**, 100, 6743.
- Corma, A.; Grande, M. S.; Gonzalez-Alfaro, V.; Orchills, A. V. *J. Catal.* **1996**, 159, 375.
- Corma, A.; Fornes, V.; Navarro, M. T.; Perez-Pariente, J. *J. Catal.* **1994**, 148, 569.
- Hunger, M.; Schenk, U.; Breuninger, M.; Gläser, R.; Weitkamp, J. *Microporous Mesoporous Mater.* **1999**, 27, 261.
- Xu, M. C.; Wang, W.; Seiler, M.; Buchholz, A.; Hunger, M. *J. Phys. Chem. B* **2002**, 106, 3202.
- Jentys, A.; Klesstorfer, K.; Vinek, H. *Microporous Mesoporous Mater.* **1999**, 27, 321.
- Busio, M.; Jänchen, J.; van Hooff, J. H. C. *Microporous Mater.* **1995**, 5, 211.
- Mokaya, R.; Jones, W.; Luan, Z.; Alba, M. D.; Klinowski, J. *Catal. Lett.* **1996**, 37, 113.
- Liebold, A.; Roos, K.; Reschtlowski, W.; Esculcas, A. P.; Rocha, J.; Philippou, A.; Anderson, M. W. *J. Chem. Soc., Faraday Trans.* **1996**, 92, 4623.
- Jänchen, J.; Stach, H.; Busio, M.; Van, Wolput, J. H. M. C. *Thermochim. Acta* **1998**, 312, 33.
- Hunger, M. *Solid State Nucl. Magn. Reson.* **1996**, 6, 1.
- Corma, A. *Chem. Rev.* **1995**, 95, 559.
- Farneth, W. E.; Gorte, R. J. *Chem. Rev.* **1995**, 95, 615.
- Rothwell, W. P.; Shen, W.; Lunsford, J. H. *J. Am. Chem. Soc.* **1984**, 106, 2452.
- Lunsford, J. H.; Rothwell, W. P.; Shen, W. X. *J. Am. Chem. Soc.* **1985**, 107, 1540.
- Chu, P. J.; Carvajal, R. R.; Lunsford, J. H. *Chem. Phys. Lett.* **1990**, 175, 407.
- Kao, H. M.; Grey, C. P. *J. Am. Chem. Soc.* **1997**, 119, 627.
- Zhao, B.; Pan, H.; Lunsford, J. H. *Langmuir* **1999**, 15, 2761.
- Bendada, A.; DeRose, E.; Fripiat, J. J. *J. Phys. Chem.* **1994**, 98, 3838.
- Kao, H. M.; Grey, C. P. *Chem. Phys. Lett.* **1996**, 259, 459.
- Kao, H. M.; Grey, C. P.; Pitchumani, K.; Lakshminarasimhan, P. H.; Ramamurthy, V. *J. Phys. Chem. A* **1998**, 102, 5627.
- Kao, H. M.; Liu, H. M.; Jiang, J. C.; Lin, S. H.; Grey, C. P. *J. Phys. Chem. B* **2000**, 104, 4923.
- Yuan, Z. Y.; Zhou, W. Z. *Chem. Phys. Lett.* **2001**, 333, 427.
- Xu, T.; Haw, J. F. *Top. Catal.* **1997**, 4, 109.
- van Eck, E. R. H.; Janssen, R.; Maas, W. E. J. R.; Veeman, W. S. *Chem. Phys. Lett.* **1990**, 174, 428.
- Beck, L. W.; White, J. L.; Haw, J. F. *J. Am. Chem. Soc.* **1994**, 116, 9657.
- Grey, C. P.; Vega, A. J. *J. Am. Chem. Soc.* **1995**, 117, 8232.
- Fyfe, C. A.; Mueller, K. T.; Grondy, H.; Woog-Moon, K. C. *J. Phys. Chem.* **1993**, 97, 13484.
- Deng, F.; Du, Y.; Ye, C. H.; Wang, J. Z.; Ding, D. T.; Li, H. X. *J. Phys. Chem.* **1995**, 99, 15208.
- Deng, F.; Yue, Y.; Ye, C. H. *Solid State Nucl. Magn. Reson.* **1998**, 10, 151.
- Fenzke, D.; Freude, D.; Frohlich, T.; Haase, J. *Chem. Phys. Lett.* **1984**, 111, 171.
- Massiot, D.; Bessada, C.; Countures, J. P.; Taulelle, F. *J. Magn. Reson.* **1990**, 90, 231.
- Bourgeat-Lami, E.; Massiani, P.; Di Renzo, F.; Espiau, P.; Fajula, A. *Appl. Catal.* **1991**, 72, 139.
- Wouters, B. H.; Chen, T. H.; Grobet, P. J. *J. Am. Chem. Soc.* **1998**, 120, 11419.
- Hunger, M. *Catal. Rev.—Sci. Eng.* **1997**, 39, 345.
- Fleischer, U.; Kutzelnigg, W.; Bleiber, A.; Sauer, J. *J. Am. Chem. Soc.* **1993**, 115, 7833.
- Grey, C. P.; Arun Kumar, B. S. *J. Am. Chem. Soc.* **1995**, 117, 9071.
- Knozinger, H.; Ratnasamy, P. *Catal. Rev.—Sci. Eng.* **1978**, 17, 31.
- Mastikhin, V. M.; Mudrakovskii, I. L.; Zamaraev, K. I. *React. Kinet. Catal. Lett.* **1987**, 34, 161.
- Deng, F.; Wang, G. X.; Du, Y. R.; Ye, C. H.; Kong, Y. H.; Li, X. D. *Solid State Nucl. Magn. Reson.* **1997**, 7, 281.
- Fitzgerald, J. J.; Piedra, G.; Dee, S. F.; Seger, M.; Maciel, G. E. *J. Am. Chem. Soc.* **1997**, 119, 7832.
- Frydman, L.; Harwood, J. S. *J. Am. Chem. Soc.* **1995**, 117, 5367.
- Stebbins, J. F.; Zhao, P. D.; Lee, S. K.; Cheng, X. *Am. Mineral.* **1999**, 84, 1680.
- Lee, S. K.; Stebbins, J. F. *J. Phys. Chem. B* **2000**, 104, 4091.